Polymer 50 (2009) 4845–4851

Contents lists available at ScienceDirect

Polymer

journal homepage: www.elsevier.com/locate/polymer

UV, Raman and XRD study of polymorphism of poly(methyl-*n*-propylsilane)

Sergey S. Bukalov [a], Yan V. Zubavichus [a], Larissa A. Leites [a,*], Julian R. Koe [b], Robert West [c]

[a] Scientific and Technical Center on Raman Spectroscopy, Institute of Organoelement Compounds, Russian Academy of Sciences, Vavilova str. 28, Moscow 119991, Russia
[b] Department of Material Science, International Christian University, Mitaka, Tokyo 181-8585, Japan
[c] Organosilicon Research Center, Department of Chemistry, University of Wisconsin, Madison, WI 53706, USA

ARTICLE INFO

Article history:
Received 3 April 2009
Received in revised form
13 August 2009
Accepted 13 August 2009
Available online 19 August 2009

Keywords:
Poly(methyl-*n*-propylsilane)
Polymorphism
UV, Raman, XRD methods

ABSTRACT

Raman, UV and XRD studies have been performed to characterize the structures of differently prepared samples of poly(methyl-*n*-propylsilane). The results demonstrate polymorphism of this polymer between T_c and T_g. At room temperature the polymer can exist in up to four modifications which comprise one amorphous disordered phase and three more ordered modifications, differing in the interchain organization and in the silicon backbone conformations. The latter are considered to be *deviant*, *transoid* and all-*anti*, respectively. The number of the modifications present and relative amount of each strongly depends on the preparation method and thermal history of the sample as well as on the molecular weight.

1. Introduction

The year 2003 was celebrated as the 50th anniversary of the modern era of polysilane chemistry. During these five decades, numerous papers have been published, their results covering a vast area of polysilane chemical and physical properties (see a special issue [1], a book [2] and reviews [3]). These articles define the extent of the field, and also the extent of the remaining challenges, which in a number of areas is the elucidation of the finer details of polysilane properties. In particular, as is noted in the reviews [3b,c], the relationship between the chain conformation and electronic properties of polysilanes as solids is not well understood and its clarification still remains an actual problem.

It was remarked in several papers devoted to the study of polydialkylsilanes, that the phase state of a polymer and kinetics of its thermochromic phase transition depend on the conditions of sample preparation and on the thermal history of the sample [3,4–9]. This dependence is very important in view of polysilane potential applications in modern advanced technologies (microelectronics, electroluminescent devices etc., see, e.g., recent papers [10–12]) and should be taken into account in order to tailor polysilane physical properties. Since different physical methods are often used to study differently prepared samples (bulk, differently obtained films of different thickness etc.) with various molecular weights, their results are, strictly speaking, not comparable. This may explain some of the discrepancies found in the polysilane literature.

We shall illustrate this general situation with the example of a well-studied [4,9,13–25] prototypical polysilane, poly(methyl-*n*-propylsilane) $[MeSi^nPr]_n$ (**1**), whose structure has been depicted [16] in a fascinating but unreal regular syndiotactic all-*anti* (formerly termed all-*trans*[1] [26]) conformation (presented in Fig. 1).

The synthesis of **1** and the UV absorption band at 306 nm of the high-molecular-weight fraction of this polymer in THF solution have been reported by one of us and co-workers in 1983 [13]. Continuous thermochromism was observed for the solution UV spectrum (a red shift from 305 to 330 nm on cooling) and was attributed to a continuously increasing relative population of *anti* conformations in the polymer backbone [14]. The structure and electronic properties of **1** have been discussed in reviews [16,17] along with those of other polydialkylsilanes in the all-*anti* conformation which were treated as σ-conjugated polymers (one-dimensional semiconductors with delocalized σ-bonds).

As was demonstrated by the combined UV, DSC, X-ray and optical microscopy methods [4,18–20,22–25], solid **1** undergoes a phase transition of order–disorder type at T_c in the interval of 35–55 °C and glassification at a T_g between −25 and −35 °C, depending on the molecular weight and thermal history of the sample. On heating, the thermochromic phase transition manifests itself as a gradual replacement of the UV band at ~325 nm by that at ~305 nm. Yokoyama and Yokoyama [4] compared the

* Corresponding author. Tel.: +7 499 135 9262; fax: +7 499 135 5085.
E-mail address: buklei@ineos.ac.ru (L.A. Leites).

[1] Thereafter we will use "*anti*" even where the original authors have used "*trans*".

0032-3861/$ – see front matter © 2009 Elsevier Ltd. All rights reserved.
doi:10.1016/j.polymer.2009.08.020

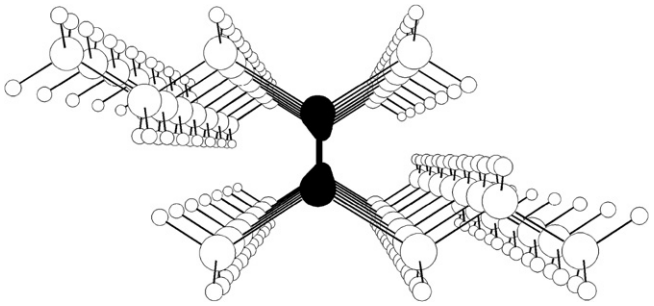

Fig. 1. Perspective end view of idealized ordered syndiotactic $[MeSi^{n}Pr]_n$ in all-*anti* conformation (reproduced by permission from the review [16]).

temperature behaviour of charge-carrier transport and of the UV absorption of solid **1** and found great differences in both mobility and UV spectra between rapidly quenched and slowly cooled samples. X-ray investigations suggested an all-*anti* conformation for the silicon chain in the ordered phase [9,19,20,22–25]. However, Asuke and West [20] reasoned that the UV absorption maximum for the low-temperature phase, 325 nm, is rather high in energy for an all-*anti* polysilane. The authors [9,23] also expressed some reservations [9,23]. In the most comprehensive paper [9], the thermal characteristics and morphology of **1** were also studied in detail. Data from optical and transmission electron microscopy, as well as X-ray scattering revealed semicrystallinity of the sample (the degree of crystallinity not exceeding 20%) and suggested lamellar structure of the microcrystals with lamellae thickness of ca. 60 Å.

Thus, analysis of the literature data presented above shows that:

1. some properties of **1**, such as thermal characteristics, charge-carrier transport and UV absorption profile, strongly depend on the thermal history of the sample and on its molecular weight;
2. the conclusion about the presence of only all-*anti* backbone conformation in the ordered part of the polymer is in some doubt, the more so that the λ_{max} value 325 nm of the corresponding UV band is in evident contradiction with an all-*anti* conformation.

The overall goals in the present study are to elucidate the reason why the properties of **1** depend on the sample thermal history, and to determine the structure of differently prepared samples of **1**, using X-ray diffraction and optical spectroscopy. To obtain strictly comparable results by different methods and thus eliminate the effect of sample preparation, we have developed a technique of obtaining uniform polysilane films and collecting UV, XRD and Raman data from the exact same sample. The latter became possible due to a recent advance in Raman instrumentation, leading to new-generation spectrometers equipped with a high-sensitivity CCD detector and a microscope.

2. Experimental section

2.1. Samples and preparation of films

Four different sets of samples of **1** were investigated. The **first set** was the same oriented fiber which was described in Ref. [23] ($M_w \approx 1.5 \times 10^4$). The fiber as-prepared could be studied only by XRD and Raman methods. In the XRD experiments, pieces of the fiber were mounted in a strictly parallel way either on a thin plate of fused quartz, or (to eliminate the contribution from quartz scattering) onto a metal ring holder. In the latter case, the pieces of the fiber were fixed in the manner of harp strings (Fig. 2) and arranged so as to align the X-ray source and the ring aperture.

Fig. 2. Schematic sketch of harp string arrangement of the fiber pieces on a metal ring holder for the XRD experiments.

The round fiber itself, "as is", could not be used for collecting UV data. Therefore we prepared a **second set** of samples from the fiber by carefully pressing it flat. This mechanical procedure, although mild, appeared to induce a change in the sample structure, leading to some disordering and to a slight redistribution in relative amounts of the polymer modifications present (see below).

The **third set** of samples correspond to thin films obtained by dissolving the same fiber in cyclohexane and subsequent film casting on a fused quartz or CsI plate. A special technique of uniform spreading of the polymer solution on the substrate surface has been developed, allowing us to obtain uniform polymer films of a given thickness. The latter varied from 3 to 0.3 μm, according to ellipsometric measurements.

The **fourth set** were films prepared in the same manner from a bulk, higher-molecular-weight ($M_w \approx 3.5 \times 10^5$) sample synthesized according to Ref. [20]. The films were cast from a solution in hexane and relaxed for a week.

2.2. Measurements

Raman spectra were obtained using T64000 and LABRAM Jobin–Yvon laser Raman spectrometers with CCD detectors for the as-prepared and flattened fiber samples as well as for the films. Spectra Physics lasers 2022 and 124 were used for spectra excitation (Ar^+ 514.5 nm and He–Ne 632.8 nm lines, respectively). To control film uniformity, Raman micro-mapping of the film surface was performed using the microscope of a T64000 instrument equipped with a TV camera.

UV spectra for the flattened fiber and film samples were recorded with a computerized M-40 Carl Zeiss spectrophotometer. Overlapping UV bands were resolved using a curve-fitting computer program assuming Gaussian and/or Lorentzian band shapes. Corrections for the background were made.

Temperature dependence of the Raman and UV spectra was measured in the interval from 80° to −190° C using specially constructed temperature cells.

XRD data were collected using an automated DRON-3 powder diffractometer in the reflection (Bragg-Brentano) focusing geometry (CuK_α radiation, $\lambda = 1.5418$ Å; 20 kV/40 mA, graphite monochromator on the secondary beam, continuous scanning mode). In room temperature experiments, very long exposure times were used (scanning speed down to 1/32 deg./min). For variable-temperature X-ray measurements (in the range of 20–60 °C), the scanning speed was 0.5 deg./min; thus, one total scan took approximately 1.5 h. XRD experiments with heating of the "as-is" fiber close to the melting point of the polymer were possible only for the samples mounted on a quartz holder. To heat the samples, a controllable flow of heated air was used. Before

each scan, the sample was kept at a given temperature for at least half an hour.

In all the variable-temperature experiments described above, the temperature was controlled by a Pt thermoresist (100 ohm) or a thermocouple with an accuracy of ±1 °C.

3. Results and discussion

3.1. UV spectroscopy

Room temperature UV spectra were obtained for numerous samples of the flattened fiber and the films prepared from the fiber solutions. The most typical spectra of both sets are presented in Fig. 3. Both bands (curves **a** and **b**), having apparent λ_{max} values at about 325 nm, evidently differ in their profiles. A shoulder on the low-frequency side at about 348 nm is clearly seen in the spectra of all the flattened fibers. An analogous well-defined shoulder at 350 nm was previously reported [4] for a broad UV absorption band of a slowly cooled film of **1**, but not for a rapidly quenched film.

Complicated UV contours obtained suggest the absorptions are superpositions of several bands. Indeed, computer curve-fitting procedures (after background subtraction) reveal three bands in the spectra of the flattened fibers (Fig. 3a) with λ_{max} values at ca. 300 (band I), 325 (band II) and 340 nm (band III) and only two of these (bands I and II, with the same λ_{max} and half-width values) in the spectra of the solution-grown films (Fig. 3b). The polymer modifications, to which these UV bands correspond, will be designated with the same Roman numerals.

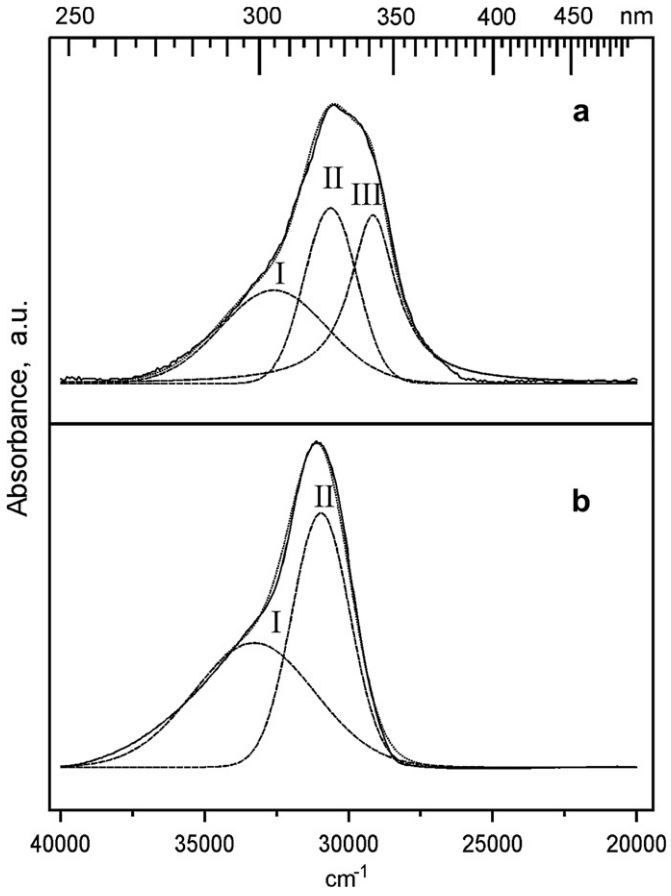

Fig. 3. UV spectra of (a) a flattened fiber and (b) a film cast from a solution of the fiber and the results of these spectra computer curve-fitting analyses after base line subtraction.

The room temperature UV spectrum of a film of a higher-molecular-weight sample of **1** (Set 4) is given in Fig. 4a. The spectrum is similar to that of the flattened fiber (Set 2) but with different relative intensities of the bands I, II and III and with a surprising addition – a weak but distinct narrow band at 378 nm (band IV, see Table 1). An analogous weak band which did not grow on further cooling has been observed previously in the UV spectrum of a polysilane $\{Si[(CH_2)_5OEt]_2\}_n$ with flexible side chains containing an oxygen atom [27].

The following band assignments are based on comparison with literature data (see reviews [3] and Refs therein). A broad UV band I at ca. 300 nm is known to belong to an amorphous state of polysilanes with disordered main chains. The UV band II at 325 nm belongs to a more ordered modification, characterized by a *deviant* (approximately7/3 helical [26]) backbone. Narrow UV bands in the region 340–350 nm are typical for the crystalline modifications of polydialkylsilanes with short alkyl substituents ($[Me_2Si]_n$ – 342 nm [28], $[Et_2Si]_n$ – 350 nm [29], $[^nPr_2Si]_n$ – 355 nm [30], $[Et^nPrSi]_n$ – 347 nm [31]). Previously they were ascribed to a planar all-*anti* conformation of the silicon chain. Now they are sometimes regarded as belonging to a near-planar *transoid* conformation, especially since recent X-ray data for model compounds (methyl oligosilanes) showed Si–Si–Si–Si dihedral angles of ~160° [32]. It is clear that band III of polymer **1** is of the same nature and we will call it *transoid*, to distinguish it from modification IV. The assignment of the UV band IV at 378 nm is unequivocal because bands in the region 370–380 nm are well-known to correspond to the longest sections of stretched silicon chains in an all-*anti* conformation which maximizes σ-conjugation within the Si backbone.

If both bands III and IV correspond to a planar all-*anti* backbone conformation, the difference between them could be explained by different higher-order polymer structures which affect the effective length of the σ-conjugated *anti*-sequences. Long chains of polysilanes with short alkyl substituents are known to pack in small lamellae with the long axis oriented perpendicular to the broad lamellar surfaces. This means that the silicon chains must be folded several times, thus reducing the effective length of σ-conjugation compared to the more extended chains characterized by the ~375 nm UV band. Other possible explanations of the difference between the UV bands at 340–350 and ~375 nm are presented in the review [3b].

It is notable that the half-widths ($\Delta\nu_{1/2}$) of the UV bands I–IV decrease with an increase in their λ_{max} (see Table 1). This means that the more ordered the polymer, the narrower is the corresponding UV absorption band. However, the exact values of λ_{max} and $\Delta\nu_{1/2}$ are noticeably temperature-dependent, and their limits are indicated in Table 1.

Thus, from the UV data it follows that the films cast from solutions of the fiber **1** (Set 3) contain only modifications I and II, the flattened fibers (Set 2) contain modifications I, II and III, while the films prepared from the higher-molecular-weight sample of **1** (Set 4) contain all the modifications I–IV.

3.2. XRD results

XRD data were obtained for the as-prepared oriented fibers, as well as for the flattened fiber samples and for the films cast from the fiber solution. For the as-prepared fiber, a clear-cut diffraction pattern of high quality is exhibited with up to 12 distinct reflections and virtually no amorphous halos (Fig. 5). In the low-angle part of this pattern, two weak reflections are clearly seen which were not reported in the previous studies. These two lines have *d*-spacings exactly double those of the most intense ones (18.57 Å and 15.08 Å, Table 2), which indicates that they cannot be due to impurities. The

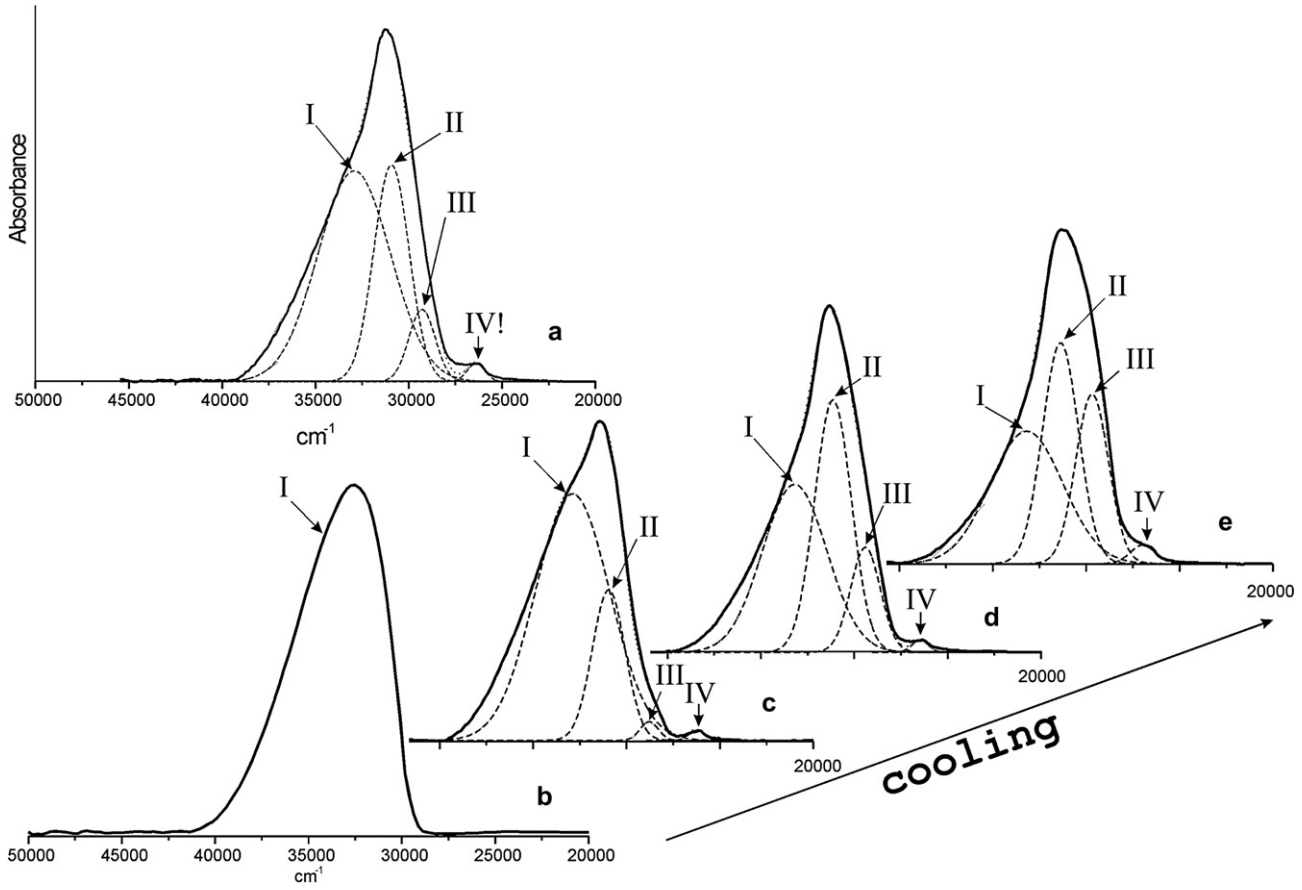

Fig. 4. Temperature evolution of the UV spectrum of a film of a higher molecular weight sample of $[MeSi^{n}Pr]_n$ and the results of these spectra computer curve-fitting analyses (see text). (a) initial film at ambient temperature; (b) above T_c; (c–e) cooling from 30° to 0 °C and −50 °C, respectively.

pattern indexing has shown that all the observed reflections are of two-dimensional character and can be fairly well indexed (see Table 2) as *hk*0 reflections of the C-centered orthorhombic cell with $a = 37.18$ Å and $b = 16.56$ Å (the parameters of the corresponding primitive unit cell are as follows: $a = 16.60$ Å, $b = 20.36$ Å, and $\gamma = 114.1$ deg.). The same parameters can be derived from those reported in Ref. [9] by doubling both translation vectors.

Since the diffraction pattern observed for the as-prepared fiber does not contain reflections with a ***c*** contribution we cannot gain any information from these data on the periodicity along the Si–Si backbone. An evident reason for the observation of only two-dimensional *hk*0 reflections could be a strongly preferred orientation of the fiber. The fiber pieces were arranged strictly parallel to the surface of the holder, so that in the *reflection diffraction geometry*, all reflections other than those corresponding to the inter-chain packing should be substantially reduced in intensity. Moreover, according to the data of Ref [9], the size of the ordered regions (lamellae thickness) along the ***c*** direction for this polymer is small (~60 Å), so only weak and broad reflections having a ***c*** contribution are expected. Thus, the assignment of all the sharp XRD reflections observed for the fiber samples to the modification with a *transoid* backbone conformation cannot be verified directly. However, a high degree of ordering is evident.

The small-angle reflections not reported by other authors are relatively weak and thus indicate a minor modification of the overall macromolecular packing, as suggested in Ref. [9] or [23]. We speculate that such a modification (*i.e.* a sort of superstructure) can include

Table 1
Ranges of the temperature-dependent values of λ_{max} and $\Delta\nu_{1/2}$ for the UV absorption bands observed in the spectra of the polymer $[MeSi^{n}Pr]_n$ between +80° and −190 °C.

	λ_{max}, nm	$\Delta\nu_{1/2}$, cm^{-1}
Band I, amorphous state, disordered backbone,	300–305	5500–4500
Band II, more ordered state, *deviant* (7/3 helical) backbone	315–325	2400–2000
Band III, crystalline state, all-*anti* or *transoid* backbone	335–353	1800–1200
Band IV, crystalline state, all-*anti* backbone	370–380	1500–1000

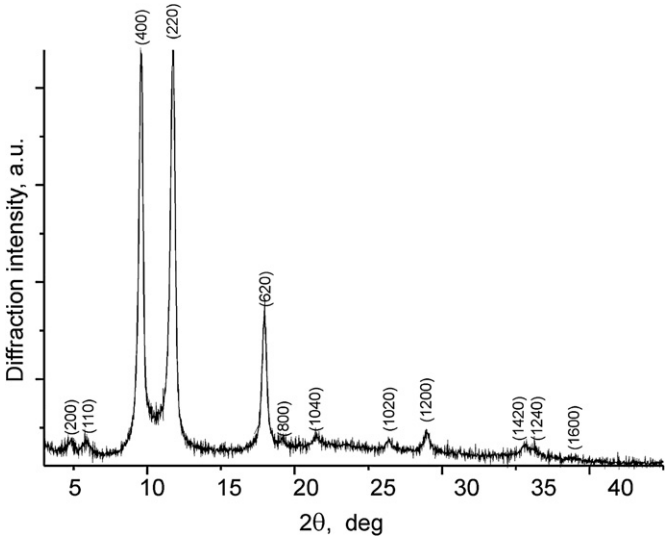

Fig. 5. XRD pattern of the oriented "as-is" fiber

Table 2
Indexing of the experimental X-ray diffraction pattern for the fiber sample.

h	k	l	$2\theta_{obs}$, deg.	$2\theta_{calc}$, deg.	d_{obs}, Å	I/I_0
2	0	0	4.75	4.75	18.574	3
1	1	0	5.86	5.84	15.081	2
4	0	0	9.50	9.51	9.300	99
2	2	0	11.65	11.69	7.590	100
6	2	0	17.85	17.87	4.964	39
8	0	0	19.12	19.08	4.638	3
0	4	0	21.44	21.44	4.141	3
10	2	0	26.23	26.26	3.395	5
12	0	0	28.79	28.80	3.098	8
14	2	0	35.50	35.47	2.527	6
12	4	0	36.17	36.18	2.482	3
16	0	0	38.71	38.71	2.324	1

a mutual rotation of the neighbouring macromolecules with the general preservation of the strict all-*anti* or *transoid* conformation of the backbones. The alternation of several differently oriented macromolecules in a unit cell could be responsible for the peculiarities in the medium-range atomic pair distribution functions reported in Ref. [23]. Room temperature XRD data for several differently prepared polymer samples (Sets 2 and 3) are shown in Fig. 6. The patterns obtained are basically similar to those reported earlier [9,20,23]. They exhibit three main, relatively narrow reflections at $2\theta = 9.50$, 11.65, and 17.85 deg. ($d = 9.30$, 7.59, and 4.96 Å, respectively), which correspond to the three most intense lines in the pattern of the as-prepared oriented fiber. However, the relative intensities of these lines vary greatly from sample to sample. Thus, it may be assumed that two distinguishable partly ordered phases are present in these samples in variable amounts. Some patterns also exhibit broad halos at 2θ values of about 10 and 20–30 deg., which could be due to a completely disordered amorphous portion of the polymer. However, proper allowance must be made for the scattering from the fused quartz sample holder which is found in the same 2θ region. Careful subtraction of the quartz pattern was made where necessary.

Of particular interest is the comparison of the UV data with the XRD results obtained for the same samples. The XRD patterns for the films of Set 3 (Fig. 6 curves 6, 7) exhibit a dominant reflection at $2\theta = 9.50$ deg., but, in contrast to those of the flattened fibers (curves 1–5), exhibit no reflection at $2\theta = 17.85$ deg. while the intensity of the reflection at $2\theta = 11.65$ deg. is strongly suppressed. A sharp reflection at $2\theta = 9.50$ deg. in that case evidently corresponds to the helical modification II with its UV band at 325 nm while those at $2\theta = 11.65$ and 17.85 deg. correspond to modification III with its UV band at 340 nm. At room temperature, the amount of modification II is large in all sets of samples. A very weak peak at $2\theta = 11.5$ deg. observed in the XRD pattern of the solution-grown films (curves 6, 7 of Fig. 6) could be due to the presence of a minor amount of modification III not apparent in the UV spectra. This contradiction may be explained by the very high sensitivity of the XRD method (which probes long-range order) to the crystalline *transoid* phase. In agreement with the UV data, two broad amorphous halos mentioned above are prominent for the films and less intense for the flattened fibers. It is notable that in the patterns of the latter (curves 1–5) their intensity varies from sample to sample.

Thus, the XRD data agree well with the UV data in that the flattened fiber samples contain three modifications whereas in the films of Set 3 only two of them are present. With progressive decrease in the overall degree of ordering, all weaker reflections (including the small-angle superstructure ones) disappear first, leaving the three most intense lines. Then only one reflection at 9.50 deg. (d = 9.30 Å) survives. A similar phenomenon, *viz.* preservation of the position of the strongest diffraction maximum after a phase transition, has been reported earlier for some polydialkylsilanes (see, *e.g.* [33]).

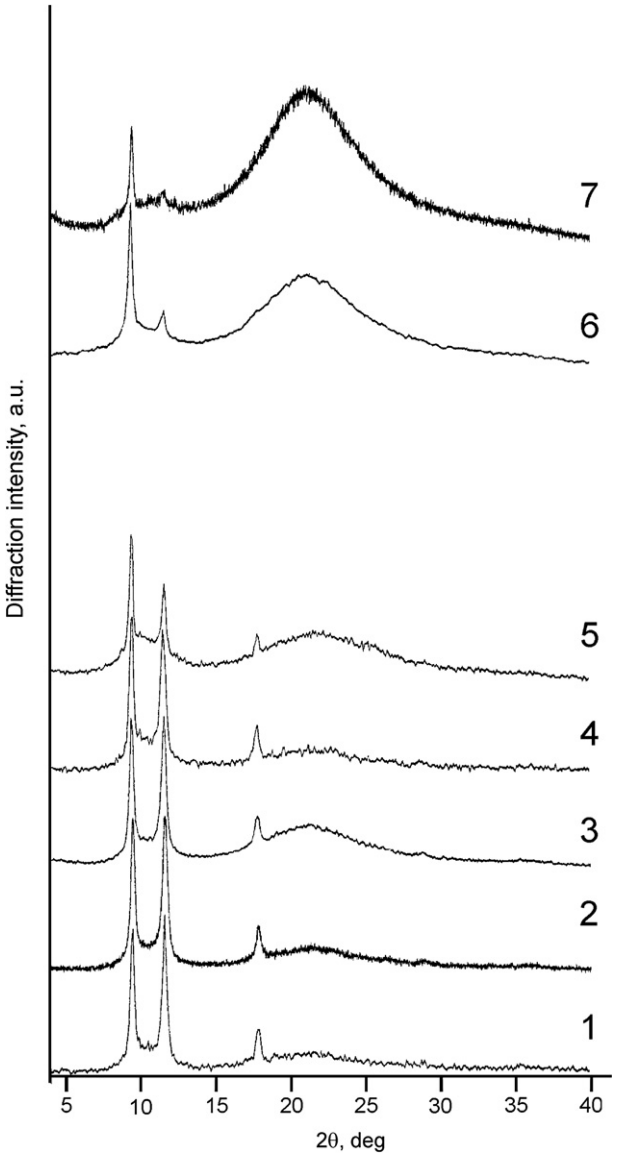

Fig. 6. XRD patterns of the flattened fiber samples (curves 1–5) and of the corresponding films (curves 6–7).

3.3. Raman spectra

Decisive evidence for the presence of the *transoid* modification III in the fiber samples and for its absence in the films of Set 3 could be gained from their dramatically different Raman spectra (Fig. 7).

In the Raman spectrum of the as-prepared fiber, in contrast to that of the corresponding film, the intensity of the lines belonging to the symmetric stretching vibrations νSi–Si at 422 cm^{-1} and νSi–C at 675 cm^{-1} is strongly enhanced and exhibits dependence on the exciting wavelength (Fig. 8). Such pre-resonance enhancement of certain Raman lines has been shown to be uniquely diagnostic of the *transoid* and *anti* conformations of the silicon chain since these are the most highly σ-conjugated [8,28,33,34]. None of the other known conformations exhibit such an enhancement. The Raman spectra of the flattened fiber samples are very similar to those of the initial fiber; however, a decrease in the amount of modification III in the

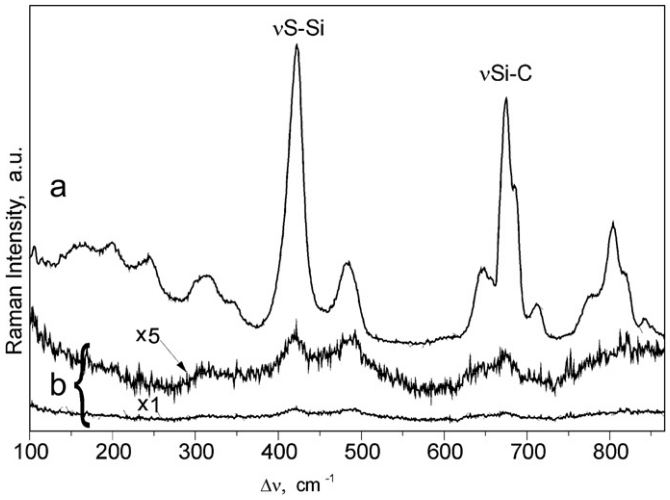

Fig. 7. Raman spectra of (a) the fiber and (b) a film cast from a solution of the fiber, λ_{exc} 632.8 nm.

former is reflected by a decrease in relative intensities of the enhanced lines.

Thus, the UV, XRD and Raman data show that the samples prepared from the fiber of **1** (Sets 1–3; $M_w \approx 1.5 \times 10^4$) can contain three different modifications: those with (a) disordered, (b) *deviant* and (c) *transoid* conformations of the backbone, the relative amount of each being prominently dependent upon preparation conditions. This is clearly seen from the different intensity ratios of the corresponding UV bands, Raman lines and XRD reflections. Fig. 6 demonstrates that the relative intensities of the reflections in the patterns obtained for five flattened fiber samples (curves 1–5) vary in repeated experiments. The "as-is" fiber does not contain an amorphous portion and has more of modification III than any other fiber samples after flattening or other mechanical or thermal treatment. The films prepared from the higher-molecular-weight sample ($M_w \approx 3.5 \times 10^5$) of **1** (Set 4) contain in addition to modifications I–III also a small amount of modification IV with an all-*anti* backbone conformation.

3.4. Thermochromic phase transition of polymer 1

As reported previously [9,18,20,23], **1** undergoes a thermochromic phase transition with T_c in the interval 35–55 °C and has a glass transition temperature T_g of ca. −30 °C. We have carried out variable temperature investigations for all the samples studied using all the techniques (UV, Raman, XRD), and the results agree well. On heating the fiber samples to T_c, all the methods demonstrate a gradual, but not parallel, decrease in the amount of modifications III and II, with the former disappearing first. This is clearly seen from Fig. 9, where the process of polymer heating is reflected by the XRD method. Above T_c, all samples exist in the disordered modification I, for which the XRD pattern contains only two amorphous halos, the UV spectrum only band I, and the Raman spectrum only broad, weak features. The process of the phase transition is also reflected in the frequency variation of the Raman line corresponding to the ν^sSi–Si mode (Fig. 10), which exhibits a typical S-shaped temperature dependence [35]. As expected, the temperature behaviour of the oriented fiber samples is not reversible. After being heated above T_c and then cooled back to room temperature, these samples contain much less of the *transoid* modification than the initial ones. This conclusion was based on the results of all the methods used and is illustrated in Fig. 9.

As another example of phase transformation in **1**, the results of variable temperature studies of the higher-molecular-weight sample (Set 4) investigated by the UV method in the interval from 80 to −40 °C are presented in Fig. 4, along with the results of computer curve-fitting analysis of the experimental contours. The initial film, whose UV spectrum is given in Fig. 4a, when heated above T_c, exhibits only band I (Fig. 4b). On cooling the sample from 45 to 30 °C, bands II, III and IV appear (Fig. 4c), the latter two with low intensity. The reappearance of band IV is of special interest. On further cooling to 0 °C (Fig. 4d), the intensity of bands II and III increases (at the expense of band I) but that of band IV does not. The reason for the low intensity of band IV at all temperatures could be as follows: polymer **1**, being atactic, cannot form perfectly ordered chains with long *anti*-sequences (such as in Fig. 1) in great amounts. Small regions with such a high degree of ordering could arise in non-equilibrium systems [36] only as a result of statistical

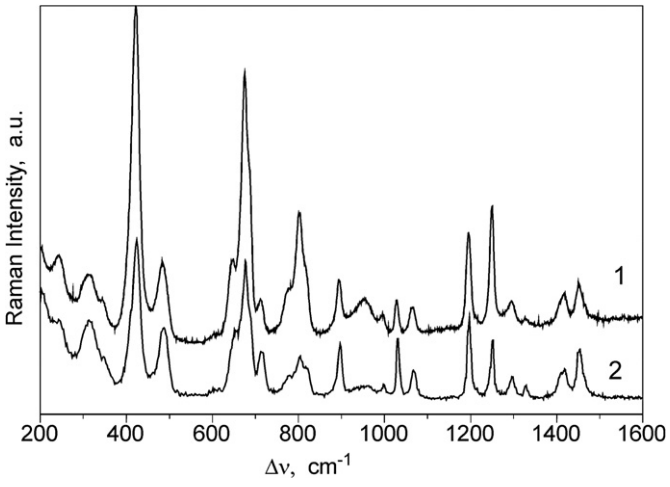

Fig. 8. Excitation dependence of the Raman spectrum of the fiber of $[MeSi^nPr]_n$ $\lambda_{exc} = 514.5$ nm (1) and 632.8 nm (2).

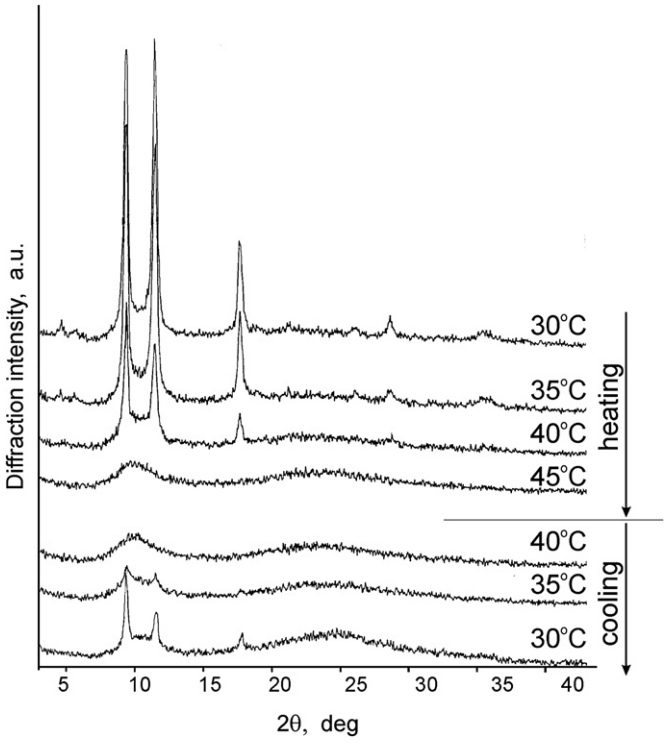

Fig. 9. XRD patterns of a fiber sample during heating and subsequent cooling.

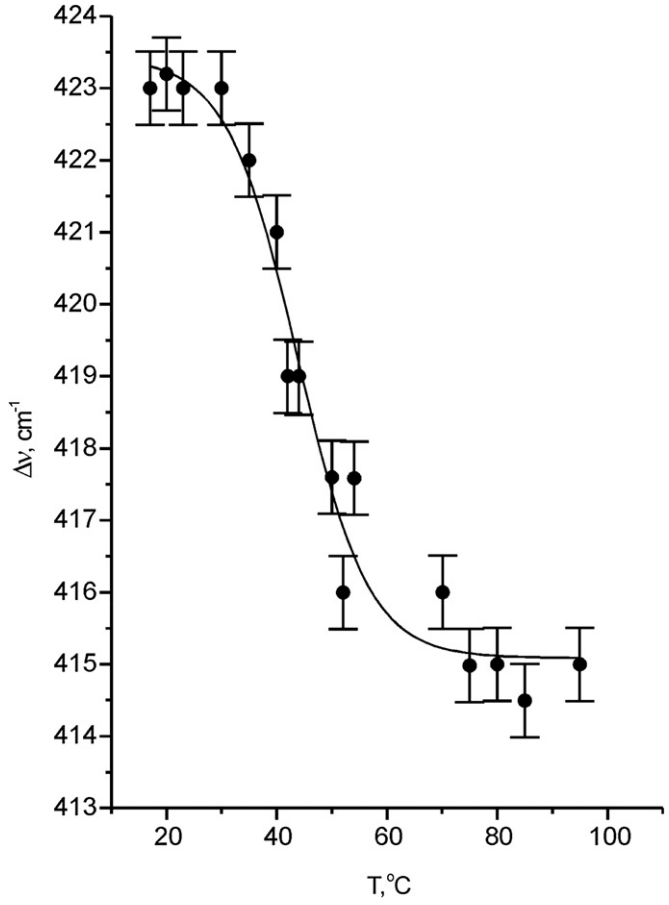

Fig. 10. S-shaped temperature dependence of the ν^{s}Si–Si mode frequency in the Raman spectrum of the fiber.

fluctuations. Between 0 °C and −30 °C, the increase in intensity of band III is the most significant (Fig. 4e). At about −40 °C, the phase transition process ceases, stopped by glassification, and the UV spectrum persists down to −190 °C, exhibiting the usual blue shift of bands III and IV on cooling (see Table 1) which is typical for ordered modifications [8a,b]. A gradual shift of the weak band IV from 381 nm at +30 °C to 369 nm at −190 °C is evident.

4. Conclusion

The results presented above unambiguously demonstrate the coexistence of several modifications (polymorphism) of polymer **1** between T_c and T_g. Four modifications: one disordered and three ordered, namely, with *deviant*, *transoid* and all-*anti* conformations of the silicon backbone could be present in the sample. The number and relative amounts of these modifications strongly depend on the preparation method and thermal history of the sample and on its molecular weight. This is the reason of contradictions revealed between the results of this polymer previous studies.

Acknowledgement

The Russian authors acknowledge partial financial support from the Russian Academy of Sciences in the framework of the program "Theoretical and experimental study of chemical bonding and mechanisms of chemical reactions and processes". The authors are indebted to M. Stchakovsky and R. Benferhat (Jobin–Yvon) for ellipsometric measurements.

References

[1] See Special Issue of J Organomet Chem 2003;685:1–2.
[2] Jones RG, Ando W, Chojnowski J, editors. Silicon-based polymers: the science and technology of their synthesis and applications. Dodrecht, The Netherlands: Kluwer Academic Publishers; 2000.
[3] For reviews see: (a) Koe JR. Organopolysilanes. In: Crabtree RH, Mingos DMP, editors. Comprehensive organometallic chemistry III, vol. 3. Elsevier Science Ltd; 2007. p. 549–650;
(b) West R. Polysilanes: conformations, chromotropism and conductivity. In: Rappoport Z, Apeloig Y, editors. The chemistry of organic silicon compounds, vol. 3. Wiley; 2001. p. 541–63 [Chapter 10];
(c) Michl J, West R. pp. 499–529 in Ref [2];
(d) West R. In: Davies AG, editor. Comprehensive organometallic chemistry II, vol. 2. Oxford: Elsevier; 1995. p. 77–109;
(e) Miller RD, Michl J. Chem Rev 1989;89:1359–410.
[4] Yokoyama K, Yokoyama M. Philos Mag B 1990;61:59–66.
[5] Kyotani H, Shimomura M, Miyazaki M, Ueno K. Polymer 1995;36:915–9.
[6] (a) Frank CW, Rao V, Despotopoulou MM, Pease RFW, Hinsberg WD, Miller RD, et al. Science 1996;273:912–5;
(b) Despotopoulou MM, Frank CW, Miller RD, Rabolt JF. Macromolecules 1995;28:6687–8.
[7] Sheiko S, Blommers B, Frey H, Moeller M. Langmuir 1996;12:584–7.
[8] (a) Bukalov SS, Leites LA, West R, Asuke T. Macromolecules 1996;29:907–12;
(b) Bukalov SS, Leites LA, West R. Macromolecules 2001;34:6003–4;
(c) Bukalov SS, Teplitsky MV, Gordeev YuYu, Leites LA, West R. Russ Chem Bull 2003;52:1066–77.
[9] Jambe B, Jonas A, Devaux J. J Poly Sci B Polym Phys 1997;35:1533–43.
[10] Ostapenko N, Kotova N, Lukashenko V, Telbiz G, Gerda V, Suto S, et al. J Lumin 2005;112:381–5.
[11] Seki S, Tsukuda S, Maeda K, Tagawa S, Shibata H, Sugimoto M, et al. Macromolecules 2005;38:10164–70.
[12] Sato T, Nagayama N, Yokoyama M. J Mater Chem 2004;14:287–9.
[13] Trefonas III P, West R, Miller RD, Hofer D. J Polym Sci Polym Lett Ed 1983;21:819–23.
[14] Trefonas III P, Damewood JR, West R, Miller RD. Organometallics 1985;4:1318–9.
[15] Takeda K, Teramae H, Matsumoto N. J Am Chem Soc 1986;108:8186–90.
[16] Matsumoto N, Takeda K, Teramae H, Fujino M. In: Zeigler JM, Fearon GFW, editors. Silicon based polymer science. Washington DC: Am Chem Soc; 1990. p. 515–41 [Chapter 28].
[17] Matsumoto N. In: Harrod JF, Laine RM, editors. Inorganic and organometallic oligomers and polymers; 1991. p. 97–113.
[18] Fujino M, Hisaki T, Fujiki M, Matsumoto N. Macromolecules 1992;25:1079–93.
[19] (a) KariKari EK, Greso AJ, Farmer BL, Miller RD, Rabolt JF. Macromolecules 1993;26:3937–45;
(b) KariKari EK, Farmer BL, Hoffmann CL, Rabolt JF. Macromolecules 1994;27:7185–91.
[20] Asuke T, West R. J Inorg Organomet Polym 1995;5:31–41.
[21] Crespo R, Tomas F, Piqueras MC. J Mol Struct (Theochem) 1996;388:285–92.
[22] Furukawa S, Koga T. J Phys Condens Matter 1997;99:L99–104.
[23] Winokur MJ, Koe J, West R. Polym Prepr 1997;35(2):57–8.
[24] Radhakrishnan J, Tanigaki N, Kaito A. Polymer 1999;40:1381–8.
[25] Furukawa S. J Organomet Chem 2000;611:36–9.
[26] (a) Michl J, West R. Acc Chem Res 2000;33:821–3;
(b) West R. J Org Chem 2003;685:6–8.
[27] Bukalov SS, Teplitsky MV, Leites LA, Yuan CH, West R. Mendeleev Commun 1996:135–7.
[28] Leites LA, Bukalov SS, Yadritseva TS, Antipova BA, Dement'ev VV. Macromolecules 1992;25:2991–3.
[29] Leites LA, Yadritseva TS, Bukalov SS, Antipova BA, Dement'ev VV. Polym Sci 1992;34:980–4.
[30] Menescal R, Eveland J, West R, Leites LA, Bukalov SS, Yadritseva TS, et al. Macromolecules 1994;27:5885–92.
[31] Li H, Yuan CH, West R, Bukalov SS, Leites LA. Proceedings of the 28th organosilicon symposium, University of Florida, 1995; p. 67.
[32] Marschner C, Baumgartner J, Wallner A. Dalton Trans 2006:5667–74.
[33] Schilling FC, Bovey FA, Lovinger AJ, Zeigler JM. Structures, phase transitions, and morphology of polysilylenes. In: Zeigler JM, Gordon Fearon FW, editors. Silicon-based polymer science. Adv in Chem Ser 224. Washington: ACS; 1990. p. 341–78 [Ch 21].
[34] (a) Bukalov SS, Leites LA, Magdanurov GI, West R. J Org Chem 2003;685:51–9;
(b) Leites LA, Bukalov SS. J Raman Spectrosc 2001;32:413–24.
[35] Iqbal Z, Owens FJ. Vibrational spectroscopy of phase transitions. New York: Academic; 1984.
[36] (a) Wunderlich B. Macromolecular physics V3. New York: Academic Press; 1984;
(b) Tager AA. Vysokomolek Soed (Polym Science, in Russian) 1988;30A:1347.